Universiteit
Leiden
The Netherlands

Parkinson's protein α-synuclein : membrane interactions and fibril structure

Kumar, P.

Citation
Kumar, P. (2017, June 27). *Parkinson's protein α-synuclein : membrane interactions and fibril structure*. *Casimir PhD Series*. Retrieved from https://hdl.handle.net/1887/50076

Version:	Not Applicable (or Unknown)
License:	Licence agreement concerning inclusion of doctoral thesis in the Institutional Repository of the University of Leiden
Downloaded from:	https://hdl.handle.net/1887/50076

Note: To cite this publication please use the final published version (if applicable).

Cover Page

Universiteit Leiden

The handle http://hdl.handle.net/1887/50076 holds various files of this Leiden University dissertation

Author: Kumar, Pravin
Title: Parkinson's protein α-synuclein : membrane interactions and fibril structure
Issue Date: 2017-06-27

6 Understanding the Peptide-Coiled-Coil Interaction of the Membrane-Fusion K/E Peptides

6.1 Introduction

All living organisms utilize membrane fusion for their normal functioning. Cellular activities that involve membrane fusion are hormone secretion, enzyme release, neurotransmission etc. Membrane fusion needs a specialized set of proteins, such as the SNARE protein complex (1–7) (SNARE: soluble NSF attachment protein receptor; NSF=*N*-ethylmaleimide-sensitive factor). Membrane fusion induced by SNARE involves the coiled-coil interaction between three complementary SNARE proteins (8).

To understand this protein-mediated membrane fusion, a coiled-coil model system mimicking the complex of SNARE proteins was designed (9,10). It performs fusion by a pair of complementary lipidated oligopeptides E/K, which contain a lipid anchor segment, a coiled-coil zipper segment, and a linker that connects the two segments (see Figure 6.1). To gain a better picture on membrane fusion, we focus on the coiled-coil zipper segment of the complex, which consists of the helical peptides K and E, for sequences see Table 6.1.

The peptides are relevant to initiate the interaction of the two membranes to be brought together, a process that relies on complementary charges of K and E, and coiled-coil formation enhanced by the knob and hole principle (see Figure 6.2). Previous studies (9, 11) have shown that the K and E peptides behave differently in solution: E, anionic in nature, is in a random coil conformation and K, cationic in nature, has some helical character and a larger tendency to self-aggregate than E.

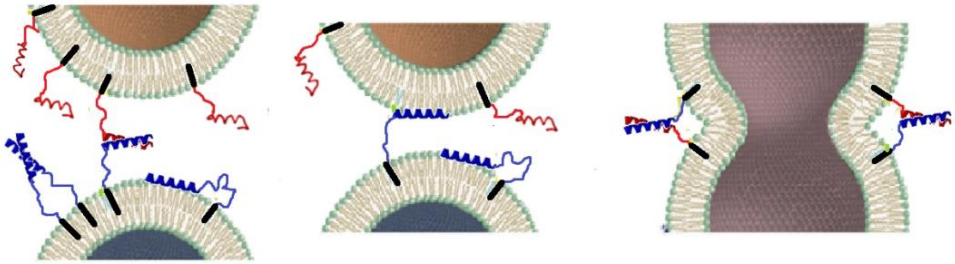

Figure 6.1. Membrane fusion model: Two membranes (top and bottom) are brought together by the lipidated peptide constructs (E/K): lipid anchor, black; PEG12 chains, the linker (for clarity drawn at the same color as the peptide); complementary peptides K, blue and E red respectively. The proposed interaction [by Rabe *et al*., (12)] of peptide K with lipid head groups is not shown.

Table 6.1. Sequence of the helical peptides E and K

Peptides	sequences
E	Ac-$(EIAALEK)_3$-GY-NH_2
K	Ac-$(KIAALKE)_3$-GW-NH_2
E-SL	Ac-$(EIAALEK)_3$-GYC(SL)-NH_2
K-SL	Ac-$(KIAALKE)_3$-GWC(SL)-NH_2
SL-K	Ac-C(SL)-$(KIAALKE)_3$-GW-NH_2

C(SL): cysteine with MTSL attached, Ac: acetyl

A new mechanism was proposed about a twofold role of the K-peptide in membrane fusion (12,14): a. to first bring the target vesicles into close proximity (≈ 8 nm) by E/K coiled-coil formation and b. to modify the head group regions of the K-peptide-binding sites at two different membranes, promoting protrusion of the lipid acyl chains as the initial state of lipid mixing. The role of K-peptide dehydration is not yet clear.

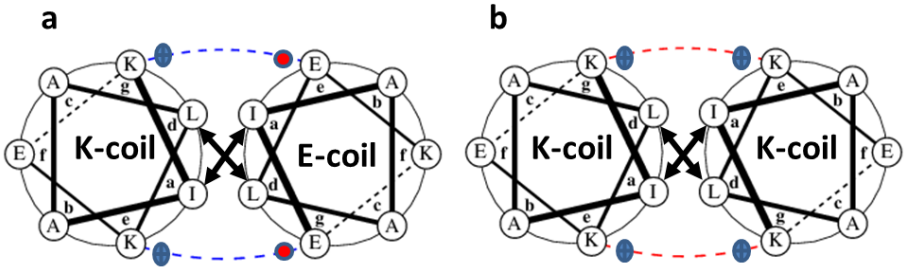

Figure 6.2. Helical wheel representation of the quaternary structure of parallel oriented (a) K/E-heterodimer and (b) K-homodimer. a, b, c, d, e, f, and g indicates the position of heptad repeats. Blue dashed line: coulomb attractions of the positively charged lysine side chains and negatively charged glutamate side chains; Red dashed line: coulomb repulsions of the positively charged lysine side chains; bold arrows: Van der Waals interactions of hydrophobic leucine and isoleucine side chains. Helical wheel projections also showing the knobs into hole model (13): Ile represents the hole; Leu represents the knob.

Circular-Dichroism (CD) experiments revealed the thermal folding, i.e., formation of α-helices of the two peptides in aqueous solution (11,15), suggesting that the proteins form helical dimers. The folding constants (K_f) were obtained for the pure E-peptides (5.3×10^2 M^{-1}), the pure K-peptides (3.4×10^3 M^{-1}) and mixtures of the E and K-peptides (1.8×10^7 M^{-1}). The folding constant for the K-peptide suggests that it forms a dimer under the conditions of the present study.

Up to now, the presence of K-homodimers and their arrangement was not proven in a more direct way. For the E/K-heterodimer, techniques like Förster resonance energy transfer (FRET) and paramagnetic proton nuclear magnetic resonance (NMR) were applied to study the orientation of the heterodimer suggesting a parallel-oriented arrangement (16). The electron paramagnetic resonance (EPR) approach used in the present study, allows measuring distances between spin labels in a self-associated complex of identical (K/K) and non-identical (E/K) peptide molecules.

Here, we investigated variants of the oligopeptides E and K, synthesized (16,17) following the original protocol developed by Litowski and Hodges (11). The two oligopeptides are oppositely charged, attain random coil (E peptides) and α-helical form (K peptides) in solution and form coiled-coil structures (11) when mixed together. The structure and the orientation of dimers are studied by continuous-wave (cw) EPR and a pulsed EPR method called double electron-electron resonance (DEER).

Similar to the results of other techniques (16,18), we detected the parallel orientation of the heterodimer of E/K peptides. In addition, we also detected the homodimers of K-peptides and their orientation.

6.2 Materials and methods

6.2.1 Peptide synthesis, labelling and sample preparation

The synthesis of the MTSL-labelled K and E peptides listed in Table 6.1 has been described elsewhere (16,17). Solutions of each peptide were prepared in PBS buffer containing 20% (wt) glycerol used as a cryo-protectant for the preparation of frozen samples listed in Table 6.2. For studying the E/K coiled-coil-complex formation the two different peptides were mixed in an 1:1 molar ratio by keeping the total peptide concentration at 0.3 mM. Peptide solutions were put into 3 mm (outer diameter) quartz tubes and then the samples were plunged into liquid nitrogen for fast freezing. The same samples were used for cw-EPR and DEER measurements.

Table 6.2. List of samples used for EPR measurements, for abbreviations see Table 6.1.

1	**E-SL**
2	**K-SL**
3	**SL-K**
4	**E-SL:K-SL**
5	**E-SL:SL-K**

6.2.2 cw-EPR measurements at 120 K

The 9.7 GHz cw-EPR measurements were performed using an ELEXYS E680 spectrometer (Bruker, Rheinstetten, Germany) with a rectangular cavity, using a modulation frequency of 100 kHz. For measurements at 120 K, a helium gas flow cryostat (Oxford Instruments, United Kingdom) with an ITC502 temperature controller (Oxford Instruments, United Kingdom) was used. The frozen samples were inserted in the pre-cooled helium gas flow cryostat. The EPR spectra were recorded using modulation amplitude of 0.25 mT and a microwave power of 0.63 mW. Typical accumulation times were 10-14min.

6.2.2.1 Simulation of EPR spectra

The spectral simulation was performed using Matlab (7.11.0.584, Natick, Massachusetts, U.S.A) and the EasySpin package (19). For all simulations, the following spectral parameters were used: g = [2.00906, 2.00687, 2.00300] (20), the hyperfine tensor parameters A_{xx} = A_{yy} = 13 MHz, and the A_{zz} parameter was varied. We used A_{zz} = 103 MHz for **E-SL** and 102 MHz for both **K-SL** and **E-SL : K-SL**. The linewidth parameter (lwpp, peak to peak linewidth in mT) was obtained from the simulation of the spectrum of a sample of MTSL in the buffer described above

and was kept fixed for the simulation of the other spectra. A traceless-dipolar tensor of the form [- D - D + 2D], in which 2D represents the parallel component of the dipolar tensor, was used. The value of D (in MHz) was varied until the simulation agrees with the experimental spectrum. By doing this we were able to obtain the dipolar frequency (in MHz), from which the corresponding inter-spin distance is calculated.

6.2.3 DEER measurements

All DEER experiments were done at 9.5 GHz on an ELEXSYS E680 spectrometer (Bruker, Rheinstetten, Germany) using a 3 mm split-ring resonator (ER 4118XMS-3-W1). We performed the measurements at 40 K with a helium gas flow using a CF935 cryostat (Oxford Instruments, United Kingdom). The pump and observer frequencies were separated by 70 MHz and adjusted as reported before (21). The power of the pump-pulse was adjusted to invert the echo maximally (22–25). The length of the pump-pulse was set to 16 ns. The pulse lengths of the observer channel were 16 and 32 ns for π/2- and π - pulses, respectively. A phase cycle (+ x) - (- x) was applied to the first observer pulse. The complete pulse sequence is given by: $\frac{\pi}{2_{\mathrm{obs}}} - \tau_1 - \pi_{\mathrm{obs}} - t - \pi_{\mathrm{pump}} - (\tau_1 + \tau_2 - t) - \pi_{\mathrm{obs}} - \tau_2 - \mathrm{echo}$. The DEER time traces for ten different τ_1 values spaced by 8 ns starting at τ_1 = 200 ns were added to suppress proton modulations. Typical accumulation times per sample were 16-20 hours.

6.2.3.1 DEER analysis

In order to analyze the DEER traces and extract the distance distributions, the software package “DeerAnalysis 2011” was used (26). All the DEER traces were corrected by a homogeneous 3D-background function, which describes the three-

dimensional random distribution of nano-objects in the sample (21-24). This approach is justified because the proteins are soluble in buffer and no membranes are present. Peptides or proteins interacting with membranes can cause lower dimensionality background functions, such as a 2D background. The distance distribution was derived by the model-free Tikhonov regularization (22–26).

6.3 Results

Figure 6.3 shows the cw-EPR spectra of spin-labelled E and K peptides measured at 120 K. We compare the spectra of all peptide samples (listed in Table 6.2) with the spectrum of MTSL, which serves as a monomeric reference for the spin label under the solution conditions used for the K/E peptides. Figure 6.3a shows the superposition of the spectra of **E-SL**, **K-SL** and a 1 : 1 mixture of **E-SL** : **K-SL** with MTSL and Figure 6.3b shows the superposition of the spectra of **SL-K** and a 1 : 1 mixture of **E-SL** : **SL-K** with MTSL. Line broadening is observed for the spectra shown in Figure 6.3a, but not for those in Figure 6.3b. These observations are summarized in Table 6.3.

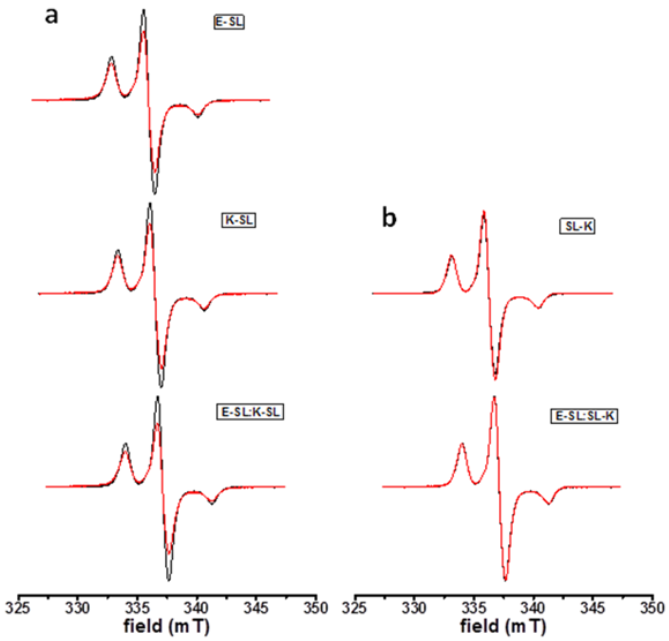

Figure 6.3. cw-EPR spectra of spin labelled E, K and coiled-coil E/K peptides at low temperature (120 K). a: Superposition of spectra of **E-SL**, **K-SL** and **E-SL : K-SL** peptides (red) is shown with the spectrum of pure MTSL (black), b: Superposition of spectra of **SL-K** and **E-SL : SL-K** (red) with the spectrum of free MTSL (black). All spectrum is normalized to the same number of spins.

Figure 6.4 shows the DEER results obtained for spin-labelled E and K peptide samples listed in Table 6.2; in Figure 6.4a the experimental DEER time traces before the background correction are displayed, in Figure 6.4b the experimental time traces after background correction with the fits corresponding to the distance distributions in Figure 6.4c. The experimental traces of **K-SL** and the 1 : 1 mixture of **E-SL** : **K-SL** (shown in Figure 6.4a) have a low modulation depth (see Table 6.3), showing that a significant population has conformations with distances outside the DEER measurement range (i.e., smaller than 2 nm or larger than 5 nm). In contrast, the modulation depth in the DEER traces of **E-SL**, **SL-K** and **E-SL** :

SL-K (see Table 6.3) shows that a significant population of spins in these samples have conformations with distances in the sensitive range of DEER.

Table 6.3. Summary of EPR properties and distances of E/K peptides

samples	cw-EPR line-broadening compared to MTSL	distance from cw-EPR spectra (nm)	modulation depth of the DEER trace	distance from DEER analysis (nm) (width (FWHM))
E-SL	yes	1.8 – 2.0	0.29	4.4 (1.6)
K-SL	yes	1.8 – 2.0	0.21	na
SL-K	no	no short distances	0.31	2.6 (1.4)
E-SL : **K-SL**	yes	1.8 – 2.0	0.22	na
E-SL : **SL-K**	no	no short distances	0.40	3.2 (1.3)

na: modulation depth too low to obtain relevant distances (see text); FWHM: full width half maximum of distance peak

The distance distribution obtained for **E-SL** is broad (full width half maximum (FWHM) 1.6 nm, see Table 6.3) with a maximum at 4.4 nm, whereas that for **SL-K** is narrow (FWHM 1.4 nm) with a maximum at 2.6 nm. The distance distribution of **E-SL** : **SL-K** is broad, suggesting that multiple conformations contribute to the distance distribution. The distance distributions for **K-SL** and **E-SL** : **K-SL** are not meaningful, because they represent only a very small population of spins in the sample (see above).

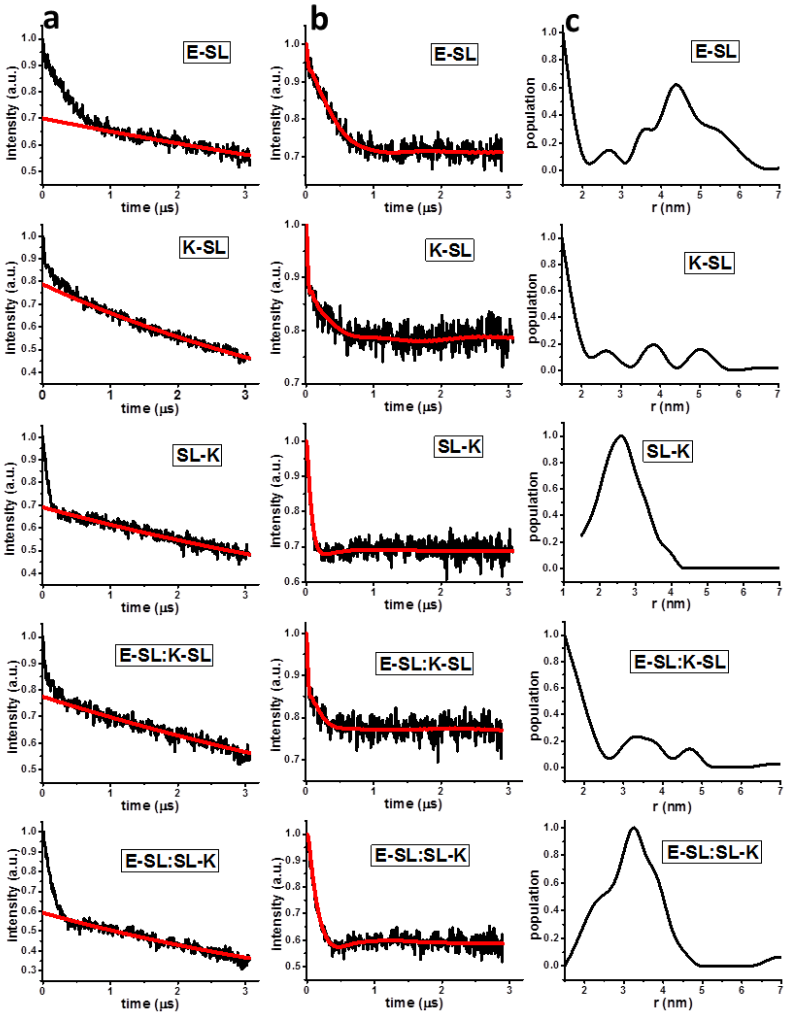

Figure 6.4. DEER results of experiments on spin labelled E and K peptides (listed in Table 6.2). a. DEER time traces before background corrections (black lines), background (red line); b. DEER time traces after background corrections (black line), fit of the time trace (red line) with the distance distributions shown in c; c. distance distributions obtained after Tikhonov regularization.

6.4 Discussion

In this study, we determine the interactions between the K- and the E-peptides by EPR using two complementary methods: Short distances (up to 2 nm) are detected by cw-EPR and longer distances by DEER. For these experiments, the peptides are investigated in frozen solution using the same sample for both types of measurements. Table 6.3 summarizes the results obtained.

The broadening of cw-EPR spectra is observed for **E-SL**, **K-SL** and **E-SL** : **K-SL** corresponds to distances in the range of 1.8 to 2.0 nm. These distances are derived from simulations of the EPR spectra (see Materials and methods). In the present samples, because of different spin-label linker conformations and the intermolecular nature of the interactions, cw-EPR line broadening most likely reflects not a single distance/conformation and therefore only a range of distances (see Table 6.3) can be derived from the broadening observed. Longer distances (> 2 nm) are detected by DEER, a method that gives the distance distributions, which reflect the distances of all members of the ensemble. Under the present experimental conditions, distances longer than 5 nm cannot be reliably detected. In DEER, the modulation depth reflects the fraction of the sample in which two spins interact within the distance range of the experiment, here 2-5 nm. Distance distributions of DEER experiments with low modulation depth, i.e., around 0.2, see Table 6.3, are not meaningful, because they are not representative of a major fraction of the spins in the sample. Using these principles we arrive at the following interpretations:

The K/E mixture shows a short distance when the C-termini of both peptides are labelled (cw-EPR) and a distance of 3.2 nm when the C-terminus of K and the N-terminus of E are labelled. The K peptide alone shows a short distance when labelled at the C-terminus and a distance of 2.6 nm when labelled at the N-

terminus, whereas E shows a broad range of distances, suggestive of unspecific aggregation.

A short distance between the two C-terminally labelled peptides (**E-SL : K-SL**) and a longer one, when one peptide is labelled at the C-terminus and the other at the N-terminus (**E-SL : SL-K**) is in qualitative agreement with a parallel heterodimer. The WebLab software (Molecular Simulations) calculations of the dimer, discussed below, qualitatively support this view.

The interaction of the spin-labels in the K-peptide is stronger for the C-terminally labelled K (**K-SL**) than for the N-terminally labelled K (**SL-K**). A distance between 1.8 nm and 2 nm for **K-SL** is only compatible with a parallel homodimer. The distance for **SL-K**, 2.6 nm, is consistent with a homodimer in which the spin labels point away from each other and possibly indicate flared-out ends of the N-terminal region of the homodimer.

In order to visualize the dimer of **E-SL** : **SL-K**, the model of the dimer has been created from WebLab software (Molecular Simulations) by assuming standard ϕ (phi) and ψ (psi) angles for a regular α helix including cysteine (SH) (both Cys-K and E-Cys). We have built the S-S bond and included the atoms required to define the MTSL label. The molecules were arranged as close as possible and in a parallel orientation (shown in Figure 6.5) to represent the quaternary structure of the E/K complex. The dimer of **E-SL** : **SL-K** with spin labels attached gives a distance of 3.5 nm in agreement with the result of DEER of a parallel heterodimer.

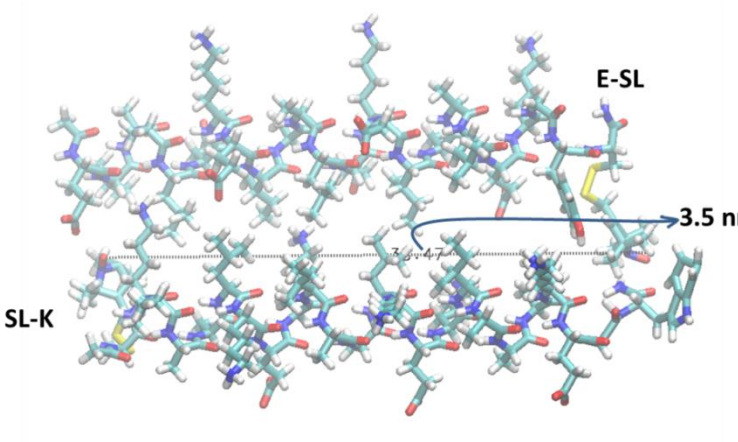

Figure 6.5. Quaternary structure of the E : K complex based on WebLab software (Molecular Simulations). Top: E-SL; Bottom: SL-K. Relative orientation: parallel with Ile and Leu oriented at the center of the E/K complex. The arrow indicates the distance between the spin labels attached to E- and K-peptide in the dimer form.

The quaternary structure of the parallel heterodimer has been also confirmed previously by different techniques (H-NMR, PRE-NMR, FRET) (16,18), and our present result is in full agreement with these results.

The finding of a K- homodimer based on DEER, in our study, was not described before.

We attribute the longer distance between the spin labels at the N-terminus (**SL-K**) to fraying of the helix ends in combination with the spin labels pointing away from each other. Distances between 1.8 and 2.0 nm at the C-terminus (**K-SL**) are consistent with the spin labels pointing towards each other. Fraying, as postulated for the N-terminus, may not be prominent for the C-terminus helix end (27,28). This is because the C-terminus contains a tryptophan residue, and could form a H-bond between the NO of the spin label and the NH proton of the indole group of the tryptophan.

The finding of a parallel homodimer for the K-peptide must be attributed to dominance of the knob-into-hole interaction (as depicted in Figure 6.2), which

overrides the unfavorable electrostatic interaction of the K-residues and the repulsive helix-dipole interaction of a parallel homodimer.

In general, we observe results that indicate K-homodimers and E/K heterodimers. The distances observed are consistent with a parallel heterodimer of the K and E peptide and a parallel homodimer of the K-peptide, in which the C-termini approach each other more closely than N-termini.

The absence of such an interaction for the E-peptides is in agreement with the previously found low tendency of the E-peptide to form dimers. The K_f of 530 M^{-1} (15) for E-homodimers would correspond to a population of 7% dimer under our conditions, which would be too low to detect. We attribute the broadened EPR spectra and the weak DEER response observed in the **E-SL** sample to unspecific aggregation.

In conclusion, we show that the EPR approach gives insight into the interaction of the K/E peptides in solution, peptides that are designed for membrane fusion. The study focused on the interaction of the peptide part of the membrane-fusion constructs, and opens the way to investigate molecular properties of the full membrane-fusion system.

6.5 References

1. Bennett M, Calakos N, Scheller R. Syntaxin: a synaptic protein implicated in docking of synaptic vesicles at presynaptic active zones. Science. 1992;257:255–259.

2. Oyler GA. The identification of a novel synaptosomal-associated protein, SNAP-25, differentially expressed by neuronal subpopulations. J Cell Biol. 1989;109:3039–3052.

3. Trimble WS, Cowan DM, Scheller RH. VAMP-1: a synaptic vesicle-associated integral membrane protein. Proc Natl Acad Sci U S A. 1988;85:4538–4542.

4. Südhof TC, De Camilll P, Niemann H, Jahn R. Membrane fusion machinery: insights from synaptic proteins. Cell. 1993;75:1–4.

5. Söllner T, Bennett MK, Whiteheart SW, Scheller RH, Rothman JE. A protein assembly-disassembly pathway in vitro that may correspond to sequential steps of synaptic vesicle docking, activation, and fusion. Cell. 1993;75:409–418.

6. Weber T, Zemelman BV., McNew JA, Westermann B, Gmachl M, Parlati F, Sollner TH, Rothman JE. SNAREpins: Minimal Machinery for Membrane Fusion. Cell. 1998;92:759–772.

7. Shi L, Howan K, Shen Q-T, Wang YJ, Rothman JE, Pincet F. Preparation and characterization of SNARE-containing nanodiscs and direct study of cargo release through fusion pores. Nat Protoc. 2013;8:935–948.

8. Burkhard P, Stetefeld J, Strelkov SV. Coiled coils: a highly versatile protein folding motif. Trends Cell Biol. 2001;11:82–88.

9. Robson Marsden H, Korobko AV, van Leeuwen ENM, Pouget EM, Veen SJ, Sommerdijk NAJM, Kros A. Noncovalent triblock copolymers based on a coiled-coil peptide motif. J Protein Chem. 2008;130:9386–9393.

10. Robson Marsden H, Elbers NA, Bomans PHH, Sommerdijk NAJM, Kros A. A Reduced SNARE Model for Membrane Fusion. Angew Chemie Int Ed. 2009;48:2330–2333.

11. Litowski JR, Hodges RS. Designing heterodimeric two-stranded alpha-helical coiled-coils. Effects of hydrophobicity and alpha-helical propensity on protein folding, stability, and specificity. J Biol Chem. 2002;277:37272–37279.

12. Rabe M, Aisenbrey C, Pluhackova K, de Wert V, Boyle AL, Bruggeman DF, Krisch SA, Bockmann RA, Kros A; Raap J, Bechinger B. A Coiled-Coil Peptide Shaping Lipid Bilayers upon Fusion. Biophys. J. 2016;111:1-14.

13. Crick FHC. The packing of α-helices: simple coiled-coils. Acta Crystallogr. 1953;6:689–697.

14. Rabe M, Schwieger C, Zope HR, Versluis F, Kros A. Membrane Interactions of Fusogenic Coiled-Coil Peptides: Implications for Lipopeptide Mediated Vesicle Fusion. Langmuir. 2014;30:7724-7735.

15. Rabe M, Boyle A, Zope HR, Versluis F, Kros A. Determination of oligomeric states of peptide complexes using thermal unfolding curves. Biopolymers. 2015;104:65–72.

16. Zheng T, Boyle A, Robson Marsden H, Valdink D, Martelli G, Raap J, Kros A. Probing coiled-coil assembly by paramagnetic NMR spectroscopy. Org Biomol Chem.

2015;13:1159–1168.

17. Zheng T. Zipping into fusion. Thesis, Leiden University Repository. 2014

18. Lindhout DA, Litowski JR, Mercier P, Hodges RS, Sykes BD. NMR solution structure of a highly sTable de novo heterodimeric coiled-coil. Biopolymers. 2004;75:367–375.

19. Stoll S, Schweiger A. EasySpin, a comprehensive software package for spectral simulation and analysis in EPR. J Magn Reson. 2006;178:42–55.

20. Steigmiller S, Börsch M, Gräber P, Huber M. Distances between the b-subunits in the tether domain of F0F1-ATP synthase from E. coli. Biochim Biophys Acta-Bioenerg. 2005;1708:143–153.

21. Drescher M, Veldhuis G, van Rooijen BD, Milikisyants S, Subramaniam V, Huber M. Antiparallel arrangement of the helices of vesicle-bound α-Synuclein. J Am Chem Soc. 2008;130:7796–7797.

22. Jeschke G. Distance measurements in the nanometer range by pulse EPR. ChemPhysChem. 2002;3:927–932.

23. Jeschke G. Determination of the Nanostructure of Polymer Materials by Electron Paramagnetic Resonance Spectroscopy. Macromol Rapid Commun. 2002;23:227–246.

24. Jeschke G, Koch A, Jonas U, Godt A. Direct conversion of EPR dipolar time evolution data to distance distributions. J Magn Reson. 2002;155:72–82.

25. Jeschke G, Polyhach Y. Distance measurements on spin-labelled biomacromolecules by pulsed electron paramagnetic resonance. Phys Chem Chem Phys. 2007;9:1895-1910.

26. Jeschke G, Chechik V, Ionita P, Godt A, Zimmermann H, Banham J, Timmel CR, Hilger D, Jung H. DeerAnalysis2006 - a comprehensive software package for analyzing pulsed ELDOR data. Appl Magn Reson. 2006;30:473–498.

27. Milov AD, Tsvetkov YD, Gorbunova EY, Mustaeva LG, Ovchinnikova TV., Handgraaf J-W, Raap J. Solvent Effects on the Secondary Structure of the Membrane-Active Zervamicin Determined by PELDOR Spectroscopy. Chem Biodivers. 2007;4:1243–1255.

28. Milov AD, Tsvetkov YD, Raap J, De Zotti M, Formaggio F, Toniolo C. Conformation, self-aggregation, and membrane interaction of peptaibols as studied by pulsed electron double resonance spectroscopy. Biopolymers. 2016;106:6–24.